JOURNAL OF MATERIALS SCIENCE **38** (2003) 1339– 1346

Characterization and adsorption properties of powders prepared from cactus pulp

G. CORRO-HERNÁNDEZ, M. P. ELIZALDE-GONZÁLEZ*
Centro de Química, Instituto de Ciencias, Universidad Autónoma de Puebla, P.O. Box J-55, Puebla, Pue. 72571 Mexico
E-mail: melizald@siu.buap.mx

M. M. DÁVILA-JIMÉNEZ
Facultad de Ciencias Químicas, Universidad Autónoma de Puebla, P.O. Box J-55, Puebla, Pue. 72571 Mexico

Two cactaceous powders, labelled CACMM1 and CACMM2, are shown to contain calcium oxalate and to consist of globular or cubosome particles. The samples were characterized by X-ray diffractometry, spectroscopic, thermic, nitrogen and water adsorption methods and compared with other organic compounds. The pore systems have been analysed from adsorption isotherms, *t*-plots and pore size distribution curves. The bioadsorbents CACMM1 and CACMM2 exhibited low specific surface area values and presented pores in the mesopore range. Composite adsorption isotherms for the binary mixtures benzene-hexane and benzene-cyclohexane on cactaceous powders have been established and revealed preferential adsorption of hexane and cyclohexane in the respective system. Also the adsorption behavior of dyes from aqueous solution was studied to complete the diversity of adsorbate molecules. Linear adsorption isotherms were obtained up to 6 mM dye equilibrium concentration.

1. Introduction

The need to improve the collection of adsorbents leads to the search of low cost solids that are effective in different areas and present environmental acceptance. Zeolites and silica gels are widely applied for water adsorption, while charcoals and other materials are preferred for the removal of organic compounds. Two phases, hybrid solids [1] obtained for example by the sol-gel method [2] and composite materials [3] have proved high catalytic activity [4] and offer without doubt also a potential adsorptivity. Properties and texture of synthetic adsorbents highly depend on the pair genesis-method [5] and their reproducibility is sometimes a hard work. Bioadsorbents are produced by nature and can be conditioned for a specific purpose by simple and reproducible treatments on one hand and on the other, analogues with similar or improved qualities can be tailored after encoding the complex chemical composition. Considerable research has been conducted to test the removal of pollutants by natural adsorbents [6, 7]. Nevertheless, an incomplete characterization of the adsorption properties obstructs from taking full advantage of the sorbent properties. For example, little information is available on the texture of sorbents prepared from natural organic wastes as pine bark [8], sunflower stalks [9], sawdust [10], bagasse fly ash [11] and rice husk [12].

Cactaceous material has been conventionally used to extract alkaloids and triterpenes, to produce stabilizers for the food industry [13] and for water-oil separators [14]. None of these investigations dealt with the application of cactus as adsorbent. During the course of our work on natural adsorbents, it was found that the cactaceous powders named as CACMM were able to adsorb water [15], organic vapours [16] and metallic ions [17]. In this paper the complete characterization and new adsorption properties of two CACMM powders is reported.

2. Experimental

2.1. Materials

Two different samples of CACMM were prepared by extracting the pulp of cactus as described in detail in [18, 19]. The samples thus obtained were dried for 3 h at 100°C under vacuum (10^{-6} mm Hg). The following organic compounds were used in this work: methyl cellulose (Aldrich CAS 9009-67-5), lignin (Aldrich CAS 8072-93-3) calcium oxalate monohydrated (Aldrich CAS 5794-28-5), benzene (Merck), hexane (HPLC Merck), cyclohexane (Baker). $A < 180$ μm fraction of methyl cellulose, lignin and calcium oxalate was prepared by sieving through an 80 mesh sieve. The dyes were used without any pre-treatment: Navy blue

*Author to whom all correspondence should be addressed.

(Colorantes Importados, S.A. de C.V.), Aniline blue, Methylene blue and Orange G (Aldrich).

2.2. Methods

Micrographs were obtained by scanning electron microscopy (SEM) using a JSM 5400 LV electron microscope. The XRD analysis was carried out with a Siemens D5000 diffractometer by using Cu K_α radiation (20 kV, 30 mA). Samples were analysed and run after calcination in oxygen atmosphere. For the IR spectroscopic study a spectrophotometer Nicolet Magna FTIR-750 was used. The free surface hydroxyl groups were determined under vacuum by the combination of D_2O exchange with infrared spectroscopy described in [20]. The weight loss curves for the samples under study were recorded on a thermogravimetric analyzer Netzch STE.

Nitrogen adsorption-desorption measurements were carried out on a Sorptomatic 1990 volumetric adsorption analyser from CE Instruments at −196°C. Prior to the measurements the samples (1 g) were degassed for 12 h in the apparatus at a temperature of 100°C. The magnitude of the surface area was calculated by applying the usual BET equation to the adsorption data, taking the average area occupied by a nitrogen molecule as 16.2 Å. Pore size distribution curves were calculated from the adsorption branch by the BJH (Barret-Joyner-Halenda) equation. Water vapour adsorption isotherms were measured gravimetrically using the desiccator method [21] at 25°C. Water vapour adsorption by samples with preadsorbed amounts of hexane was measured by firstly saturating the evacuated solid with hexane vapour in a desiccator. Adsorption of the binary mixtures benzene-hexane and benzene-cyclohexane was studied by direct immersion of the solids into the solutions maintained in sealed cells thermostated at 25°C during 24 hours. Analysis of the liquid mixtures after contact with the solids was performed by gas chromatography using a Shimadzu 14A chromatograph.

Dyes adsorption isotherms were measured at 25°C by high performance liquid chromatography (HPLC) using diode array detection. Navy blue and aniline red were chromatographed on a ODS2 Phase Sep (150 × 4.6 mm) column using 18% methanol-water, methylene blue on a ISCO QA (250 × 5 mm) and 20% methanol-water and Orange G on a S5P Phase Sep (150 × 4.6 mm) column and 30% methanol-water as mobile phase. A Constametric III pump and a Waters 994 photodiode array detector were used for this purpose.

3. Results and discussion

3.1. Morphological, thermic and spectroscopic characterization

In an earlier work [15] a honeycomb-like structure for the surface of CACMM1 particles has been reported. When examining sieved fractions of CACMM1 and CACMM2 with mean particle diameter 350 μm by SEM (Fig. 1), it could be observed that the CACMM1 particles had a globular and that the CACMM2 had a cubosome shape associated with them, although both materials were extracted from the same rough material but varying the extraction procedure [18]. The SEM images showed also that the CACMM2 particles have definite crystal faces. The known habit of plants to form and accumulate biominerals could support this observation. The X-ray diffraction pattern of this sample is shown in Fig. 2. Diffractogram (a) is essentially identical with that reported [22] for calcium oxalate dihydrate $C_2CaO_4 \cdot 2H_2O$. The particles maintained their form after calcination at 200°C and diffractogram (b) corresponded to $C_2CaO_4 \cdot H_2O$. The stepwise calcination procedure together with the diffractograms established the identity of the following products after each thermic reaction, where lettering in parentheses corresponds with the diffractograms in Fig. 2:

$$C_2CaO_4 \cdot 2H_2O\,(a) \xrightarrow{200^\circ C} C_2CaO_4 \cdot H_2O\,(b) \xrightarrow{400^\circ C}$$

$$CaCO_3 + CO\,(c) \xrightarrow{600^\circ C, 800^\circ C} CaO + CO_2\,(d, e)$$

At the final temperature of 800°C the powder presented however a mass lost of only 62% indicating the presence of other constituents. Diffractograms in Fig. 2 of the powders calcined at 600°C and 800°C presented lines assigned to $Ca(OH)_2$ (marked with an asterisk) due to the hydratation of CaO under the measurement conditions.

A detailed thermal study was then carried out under a dry inert atmosphere for CACMM2. Differential thermal curves of a CACMM2 sample are compared in Fig. 3 with those of calcium oxalate, methyl cellulose and lignin, which were considered by us as possible constituents of CACMM2. Probably three distinct regions of weight loss occur in CACMM2 with temperature (Fig. 3a), associated with the three observed effects in the DTA curve. The transitions temperatures are indicated in the curves. The principal finding was the fact, that for CACMM2, the DTA pattern did not match the monohydrate calcium oxalate curve (Fig. 3b). The endothermic process taking place at 250°C (loss of water of crystallization) in calcium oxalate seems to be compensated with an exothermic peak at 275°C arising from the cellulosic-lignin components in CACMM2. In $CaC_2O_4 \cdot H_2O$ the peaks at 465°C, 490°C and the preceding shoulder are responsible for the reaction:

$$CaC_2O_4 \xrightarrow{490^\circ C} CaCO_3 + CO$$

In CACMM2 the peak due to liberation of CO appears shifted to 550°C and may state the decomposition of organic moieties. Fig. 3c and d show the DTA curves of reagent grade methyl cellulose and lignin, respectively. Since cellulosic and lignin constituents of CACMM2 are not reagent grade cellulose and lignin, but natural polymers in form of guaiacyl or syringyl lignin for example, the DTA curve of CACMM2 does not present exactly the cellulose and lignin peaks. It is known that depending on the structure of cellulose and on the quantitative ratio of the structural units in lignins [23] endo- and exothermic effects can shift or split.

Early investigation of CACMM1 [15] assigned IR bands to calcium oxalate, lignin and cellulose though a

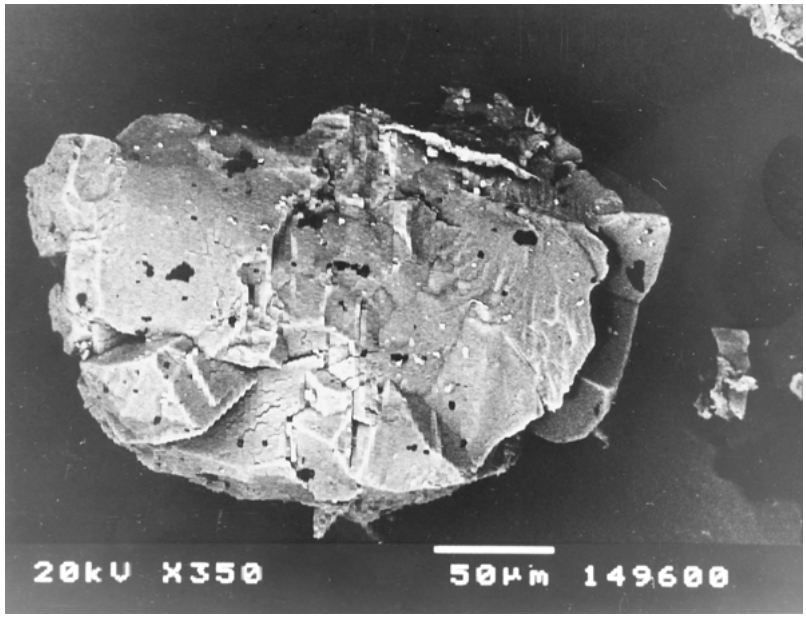

(a)

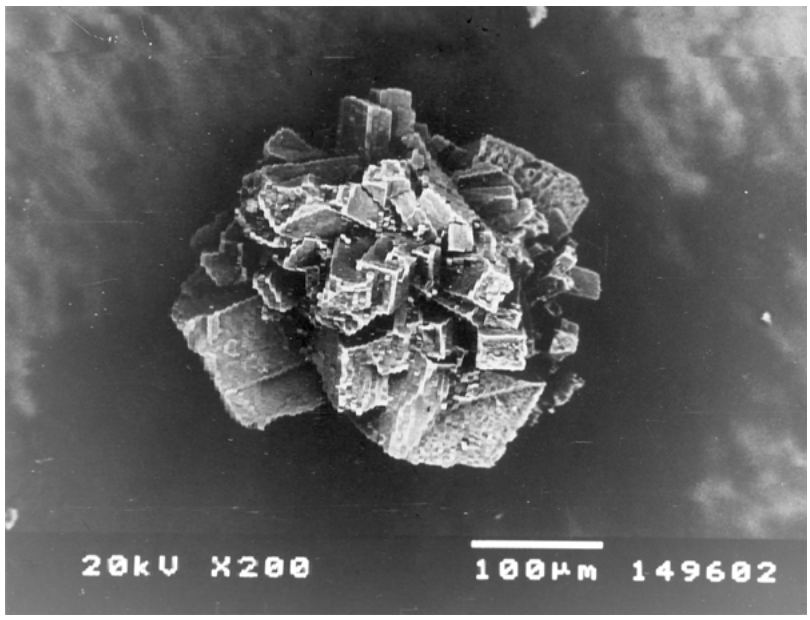

(b)

Figure 1 Surface aspect by SEM of the cactaceous powders CACMM1 (a) and CACMM2 (b).

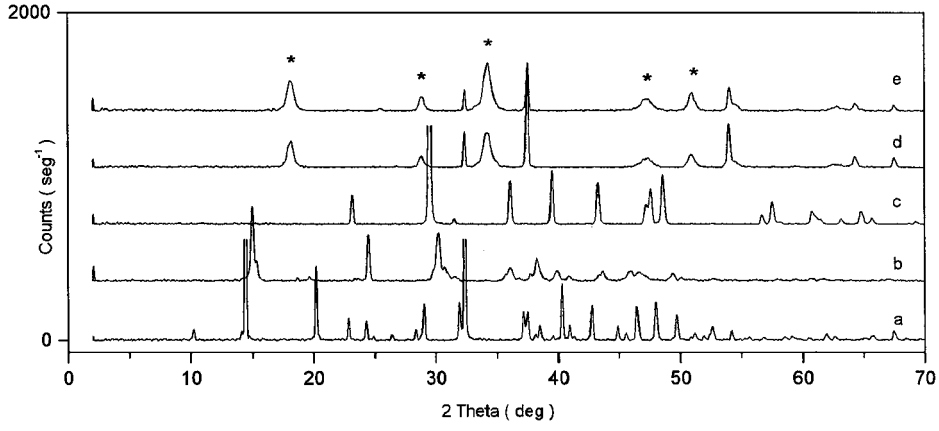

Figure 2 X-ray diffractograms of CACMM2 before thermal treatment (a) and calcined at 200°C (b), 400°C (c), 600°C (d) and 800°C (e).

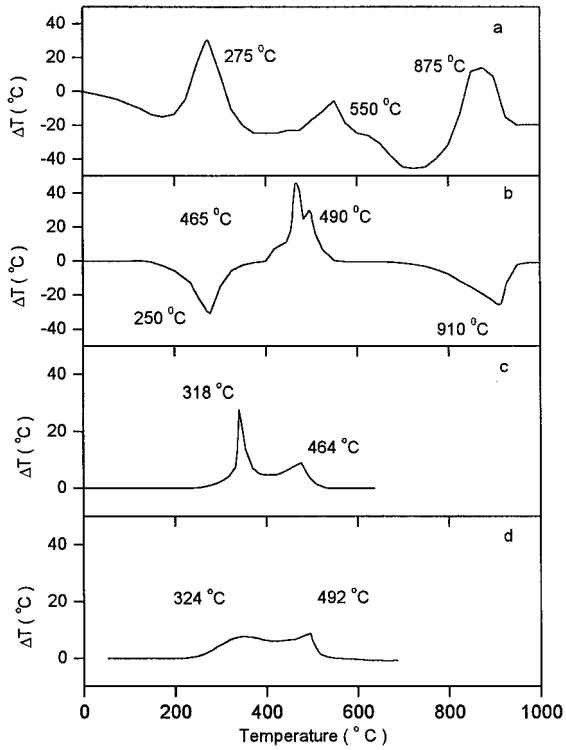

Figure 3 DTA curves of CACMM2 (a), $Ca(COO)_2 \cdot H_2O$ (b), methyl cellulose (c) and lignin (d).

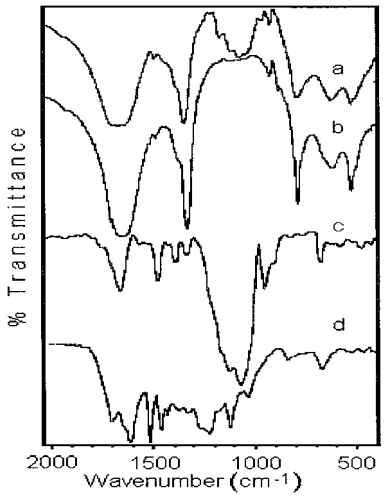

Figure 4 IR spectra of the adsorbents CACMM1 (a) and CACMM2 (b), methyl cellulose (c) and lignin (d).

high degree of band overlapping. When comparing the two CACMM samples exhibiting different morphology as demonstrated above by SEM, the quantitative spectroscopic result showed also some difference. Here both CACMM1 (Fig. 4a) and CACMM2 (Fig. 4b) present the calcium oxalate bands in the low wavelength region (517, 614 and 785 cm^{-1}), but CACMM2 does not exhibit the 1031 cm^{-1} band corresponding to the aromatic C-H in plane deformation, guaiacyl-type vibration in lignin and the 1062 cm^{-1} band of the C-O deformation vibrations in cellulose (Fig. 4c). Since characteristic bands of lignin at 1325, 1370, 1515, 1675 cm^{-1} [24] and of methyl cellulose at 1460 and 1648 cm^{-1} could be overlapped by the 1253 and 1688 cm^{-1} bands of calcium oxalate, spectra subtraction was performed, obtaining for both CACMM solids reported here one

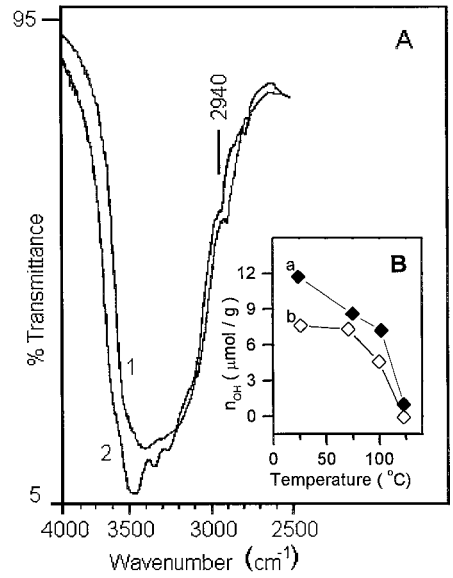

Figure 5 IR band of associated OH at room temperature and atmospheric pressure (A) and hydroxyl concentration decrease with temperature (B) of the adsorbents CACMM1 (a) and CACMM2 (b).

band corresponding to lignin at 1324 cm^{-1} and one to cellulose at 1650 cm^{-1}. In CACMM2 the subtracted bands were less intense than in the CACMM1 sample, nevertheless the vibration corresponding to an organic moiety could also be found in CACMM2. This argument is also supported by the fact that the shoulder at 2940 cm^{-1} corresponding to the C-H stretching vibration could also be seen in the infrared spectrum (Fig. 5). The broad band of the OH stretching vibration mode at 3100–3800 cm^{-1} comprises both free and hydrogen bonded hydroxyl groups. An attempt to determine the variation of the free hydroxyl groups fraction (at $\nu = 3750$ cm^{-1}) with temperature was done. At room temperature the values 12 μmol g^{-1} (0.5 μmol m^{-2}) and 8 μmol g^{-1} (0.7 μmol m^{-2}) were obtained for CACMM1 and CACMM2, respectively. These values amounted approximately one tenth of the hydroxyl groups on the hydrated silica surface (7–9 μmol m^{-2}) [25]. The insert in Fig. 5 also shows a similar but not identical diminution of the free hydroxyl groups in the CACMM samples with temperature, which practically disappear at 125°C when on the DTA curves no inflexion was appreciable.

3.2. Textural characterization

Nitrogen adsorption isotherms are shown in Fig. 6. The isotherms are not unambiguously of type III (according to the IUPAC classification [26]), for they are concave to the pressure axis in the very low pressure region, so that there is a just detectable point of inflection. The isotherms are therefore in a sense intermediate between types II and III. Type II isotherms are characteristic of non-porous solids, where the surface is wholly external, whereas type III isotherms result from adsorption on non porous or porous solids containing pores in the macropore range. Although all nitrogen adsorption isotherms could be approximately considered of type III, starting with CACMM1 (see Table I) the C constant values in the BET equation [26] are

TABLE I Surface charateristics of the studied samples

Sample	S_{BET} ($m^2\,g^{-1}$)	C_{BET}	V_p ($cm^3\,g^{-1}$)	S_t ($m^2\,g^{-1}$)
CACMM1	22	2	1	10
CACMM2	11	6	0.2	6
Methyl cellulose	0.5	13	0.4	0.3
Lignin	6	103	0.5	6
Calcium oxalate	5	43	0.1	5

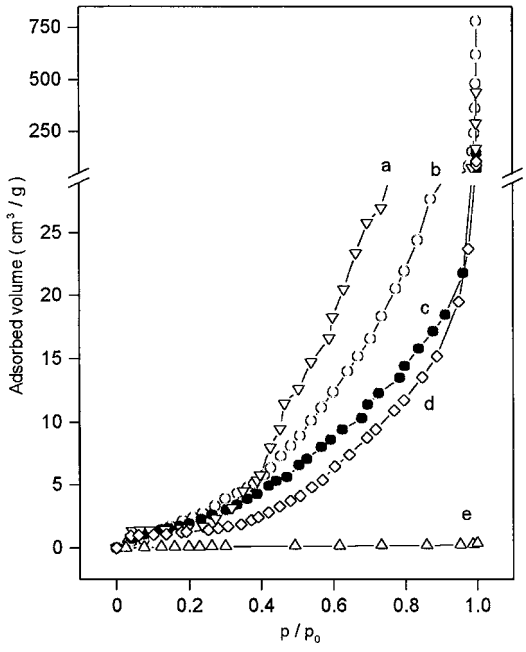

Figure 6 Nitrogen adsorption isotherms of lignin (a), CACMM1 (b), CACMM2 (c), calcium oxalate (d) and methyl cellulose (e).

slightly greater than the maximum value $C < 2$, permissible for a type III isotherm. So CACMM1 nitrogen adsorption isotherm was considered as intermediate between type II and type III isotherms, while the rest were considered as type II isotherms. In this way, specific surface was calculated for CACMM1 from the monolayer capacity as suggested for type III isotherms [26] at $(p/p_0)_m = 0.41$ and for the rest of the isotherms, as normally, at $(p/p_0)_m = 0.3$. Nevertheless, with $C < 10$ an uncertainty in the value of the specific surface as high as 100% can be expected. The BET specific surface area and the total pore volume values are listed in Table I. These magnitudes showed firstly that the studied solids exhibit low specific surface and secondly, that there are marked differences between CACMM solids and calcium oxalate, lignin and cellulose. CACMM2 specific surface is half that of CACMM1. Normally organic materials tend to have low C values. In this case lignin presented however the highest C value and could influence, if present in the CACMM solids, the adsorption isotherm form and texture characteristics as demonstrated for the silica-lignin composite [27].

Further the experimental isotherms were transformed into t-plots, where t is the standard multilayer thickness on the reference non-porous material at the corresponding relative pressure p/p_0, according to Lippens and de Boer [28]. The t-plots applied to the adsorption isotherms shown in Fig. 6 are given in Fig. 7.

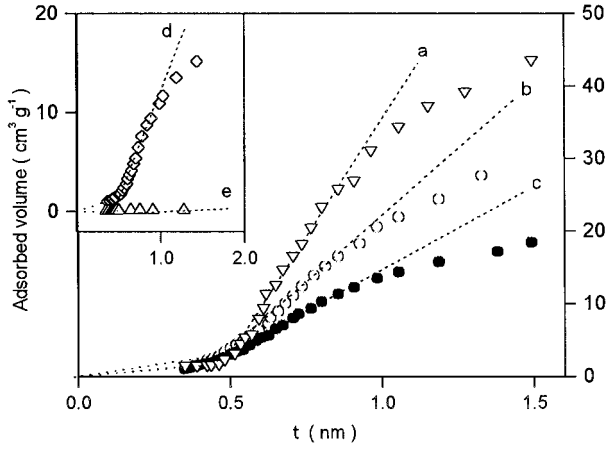

Figure 7 t-plots of the nitrogen adsorption isotherms of lignin (a), CACMM1 (b), CACMM2 (c), calcium oxalate (d) and cellulose (e). Curves a-c: right y-axis, curves d and e: left y-axis.

The standard thickness $\sigma = 0.354$ nm of the nitrogen adsorbed layer was used. The t-plot of all samples showed a straight line passing through the origin and can be divided into three parts. After the initial linear region passing through the origin deviation in an upward direction occurs, demonstrating capillary condensation in micropores of certain shape. This fact leads to a contradictory result in spite of the assumption that the materials have a microporous structure and should have presented type I adsorption isotherms. Although calcium oxalate and cellulose present half of the adsorbed volume, they bend near the t-region of 0.6 nm (at $p/p_0 = 0.44$) to give steeper slopes indicating that capillary condensation takes place. A downward deviation from the straight line at the end of the second linear region is observed at t-value 1.0 nm (at $p/p_0 = 0.78$) indicating that capillary condensation at wedge shaped pores is only possible at higher relative pressures. There are two possibilities to explain this feature: the solids have a smooth surface or micropores could be due to interstices between crystallites. The SEM images of CACMM1 and CACMM2 particles in Fig. 1 showed a quite different morphology, but no porosity or smoothness was appreciable at that magnification. The specific surface calculated by the BET equation S_{BET} was larger than the specific surface evaluated by the t-method S_t for the CACMM samples (the ratio $0.4 < S_t/S_{BET} < 0.5$), but they are in good agreement for calcium oxalate, lignin and methyl cellulose since the calculated C constant was $C > 10$. As commonly concluded for type III isotherms and low C values, S_t is a better value than S_{BET}. In general, the small S_{BET} measured in all cases indicates the presence of smooth surfaces. However, a further analysis of porosity was intended. When nitrogen desorption was measured, all the samples exhibited a very small and similar hysteresis loop (not shown in this paper) of type H3 according to IUPAC recommendations indicating slit shaped pores or planar particles. The calculated pore size distribution curves are shown in Fig. 8. CACMM1 presented a bimodal pore size distribution, that consisted of 34% pores with radius between 2 nm and 5 nm and 66% pores with overlapping sizes between 5 nm and 400 nm. CACMM2 presented a homogeneous pore size

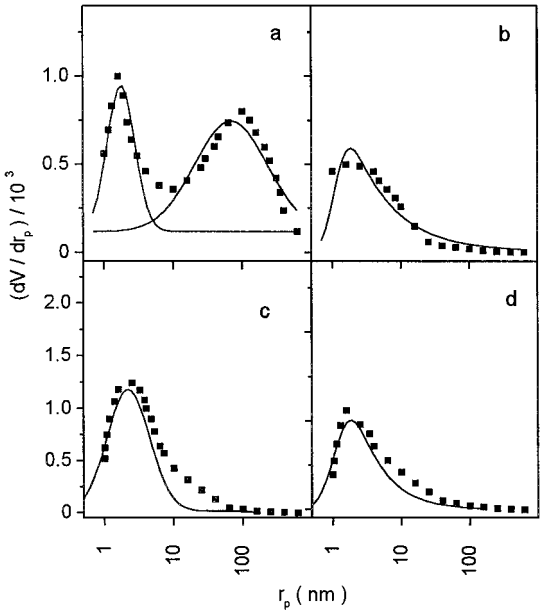

Figure 8 Pore distribution curves of CACMM1 (a), CACMM2 (b), lignin (c) and calcium oxalate (d). Experimental values (points) and adjusted curves (lines).

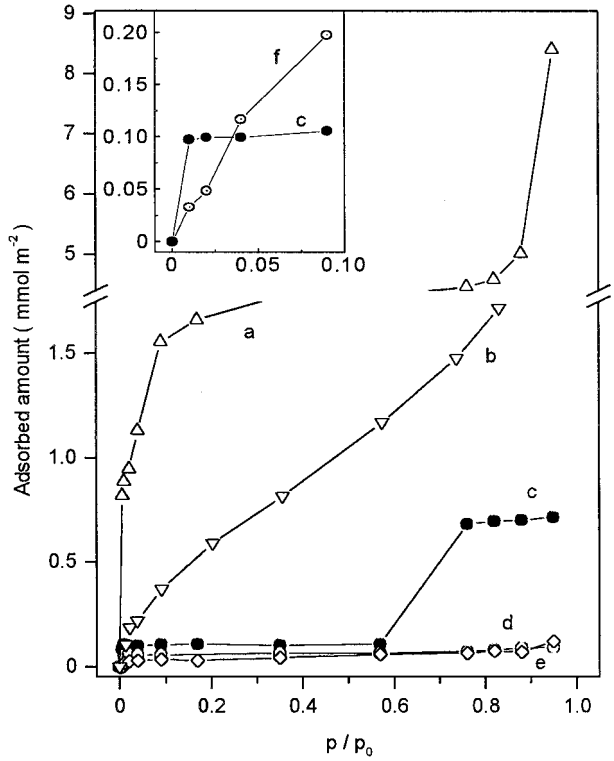

Figure 9 Water vapour adsorption isotherms at 25°C by methyl cellulose (a), lignin (b), CACMM2 (c), CACMM1 (d) and calcium oxalate (e). In the inset CACMM2 before (c) and after (f) hexane preadsorption.

distribution with radius in the range 1–100 nm. Thus, it was concluded that the samples under study exhibit meso and macropores. The distribution profiles are broad and non-symmetric and the average pore size diameter was mostly in the mesopore range: CACMM1-4 nm, lignin and calcium oxalate-5 nm, CACMM2-6 nm. The smallest pores with 4 nm diameter already correspond with small mesopores according to the IUPAC classification that considers the mesopore range starting at 2 nm. The first profile in CACMM1 and in CACMM2 look like the pore distribution curve in lignin and in calcium oxalate. Thus the second profile in CACMM1 could be attributed to the cellulosic component. However, additional work is needed to confirm this statement. The case of the CACMM1 bimodal distribution presenting meso and macropores (with average pore size of 140 nm) as well as the curves with one maximum but high tailing in the region of larger pores can explain the third downbending region in the t-curves (see Fig. 7).

3.3. Adsorption properties

As it can be seen from Fig. 9, all the studied CACMM solids demonstrated similar affinity for water. In general all water vapour adsorption isotherms are of the IUPAC type II, thus similar to those depicting water adsorption on silica gels. Exception was CACMM2 that exhibited a type IV isotherm. However, the specific adsorption given in Fig. 9 for cellulose and lignin is markedly higher in comparison with that for calcium oxalate and for the CACMM solids. The isotherm for CACMM1 runs very close to that for calcium oxalate, but CACMM2 isotherm clearly differs in type and adsorption capacity for water. A further water adsorption investigation in the relative pressure range $0.01 < p/p_0 < 0.10$ on CACMM2 after preadsorption of hexane (inset in Fig. 9) was carried out. As known, n-alkanes penetrate micropores and desorb at considerable high temperatures. Preadsorption is in this manner a method which can show a type I isotherm when it is masked by a type II isotherm. In this case, it was observed however, that in this relative pressure range the water vapour adsorption isotherm had a type I form before hexane preadsorption and turned a type II isotherm after hexane preadsorption as it is shown in detail in the inset in Fig. 9. This could be associated with a composite surface, which is partly hydrophilic, partly hydrophobic.

In our previous work [15, 16] on CACMM, we reported the adsorption of organic vapours by these natural solids. Now, we studied two binary liquid mixtures: benzene-hexane and benzene-cyclohexane. Reduced surface excess isotherms are presented in Fig. 10. Both CACMM solids presented very close negative adsorption for benzene (Fig. 10A) and respectively positive type I isotherm according to Schay and Nagy classification for hexane. This indicates that hexane with a critical diameter $d_{cr} = 0.49$ nm is preferentially adsorbed over the total concentration range probably due to a sieve effect with benzene ($d_{cr} = 0.6$ nm). When we analysed the nature of the isotherms for the mixture benzene-cyclohexane (Fig. 10B) adsorption was competitive and quite different in the system containing CACMM1 in comparison with CACMM2. On CACMM1 benzene presented a negative adsorption isotherm indicating a preferential adsorption of cyclohexane ($d_{cr} = 0.61$ nm). Since both adsorbates have practically the same critical diameter, no sieve effect can be argued and the ability of benzene and cyclohexane to undergo specific and non-specific interactions, respectively can be responsible for this behavior. On the contrary, benzene adsorption was positive within a defined concentration

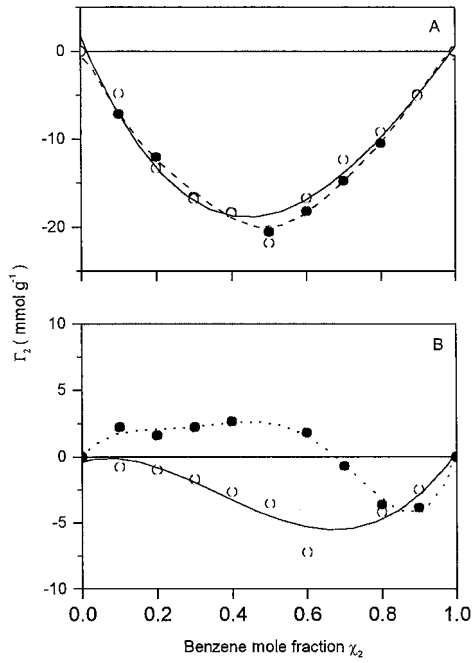

Figure 10 Adsorption of the binary mixtures benzene-hexane (A) and benzene-cyclohexane (B) on the adsorbents CACMM1 (open circles) and CACMM2 (full circles).

range on CACMM2, which corresponds with a type V isotherm. Positive adsorption of benzene in mixtures with hydrocarbons, both on hydrophilic and hydrophobic adsorbents has commonly been observed [29]. In this case the weak positive adsorption and the negative adsorption behaviour starting at $\chi_2 = 0.67$ of the mixture benzene-cyclohexane looks like the adsorption of the mixture benzene-hexane on graphitised thermal black. This proves the non-specific character of some sites on the surface of CACMM2.

At last the adsorption of dyes on CACMM2 was examined. Adsorption is characterized by linear isotherms in the studied concentration range (see Fig. 11). Both cationic dyes Navy blue and Methylene blue (curves a, b) exhibited almost the same adsorption extent. Since the slope of the lines is an indication of the relative adsorbability of the dye, we can see that the interaction with ionic dyes was favoured in comparison to π-electronic systems in the azo dyes Aniline blue and Orange G (curves c, d). This behavior can account for

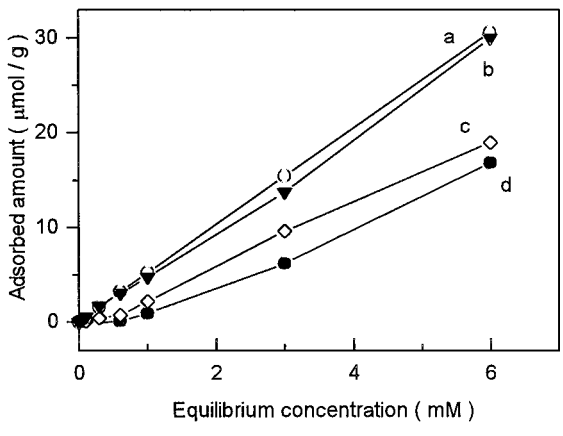

Figure 11 Adsorption isotherms of dyes solutions on CACMM2: Navy blue (a), methylene blue (b), Aniline blue (c) and Orange G (d).

the occurrence of ionic active sites capable of coulombic interactions on the surface of CACMM2. The linearity of the isotherms provides the interpretation of constant distribution of the dye between the surface layer and the bulk phase. With this set of adsorbates we could demonstrate that CACMM solids are also able to adsorb complex organic molecules from solution.

4. Conclusions

A general conclusion is made concerning the qualitative composition of the studied adsorbents. CACMM1 and CACMM2 contain in different extent calcium oxalate dihydrate and a lignin-cellulosic component responsible for the hydroxylated character of the surface, which allowed water adsorption in a measurable extent. As a result of the textural characterization, the conclusion was made that both CACMM samples exhibit low surface area magnitude due to the fact that CACMM1 presents meso and macropores, but CACMM2 a major content of mesopores. The bifunctional nature of the surface of CACMM2 containing non-polar sites as well as a polar character was evidenced by the composite isotherms of binary organic mixtures and by the adsorption of cationic dyes from aqueous solutions. From these results it can be concluded that the complex nature of the CACMM2 powders can be exploited to adsorb different kinds of chemical substances, varying in size and polarity.

Acknowledgements

The authors thank Ing. L. Baños (Instituto de Materiales, Universidad Nacional Autónoma de México) for her help in X-ray analysis, Prof. N. Alonso-Vante (University of Poitiers, France) for his help in thermic analysis and the German Society for Technical Cooperation (GTZ) for the donation of the diode array detector under grant No. 9224.

References

1. J. MROWIEC-BIAŁOŃ, A. B. JARZĘBSKI, A. I. LACHOWSKI, J. J. MALINOWSKI and Y. I. ARISTOV, *Chem. Mater.* **9** (1997) 2486.
2. H. D. GESSER and P. C GOSWAMI, *Chem. Rev.* **89** (1989) 765.
3. M. M. DÁVILA, M. P. ELIZALDE, M. GONZÁLEZ and E. GARCÍA, *J. Electrochem. Soc.* **144** (1997) 263.
4. M. SCHNEIDER and A. BAIKER, *Catal. Rev.-Sci. Eng.* **37** (1995) 515.
5. Q. HUO, J. FENG, F. SCHÜTH and G. D. STUCKY, *Chem. Mater.* **9** (1997) 14.
6. L. C. MORAIS, O. M. FREITAS, E. P. GONCALVES, L. T. VASCONCELOS and C. G. GONZÁLEZ BECA, *Wat. Res.* **33** (1999) 979.
7. S. E. BAILEY, T. J. OLIN, R. M. BRICKA and D. D. ADRIAN, *ibid.* **33** (1999) 2469.
8. S. AL-ASHEH and Z. DUVNJAK, *Sep. Sci. Technol.* **33** (1998) 1303.
9. G. SUN and W. SHI, *Ind. Eng. Chem. Res.* **37** (1998) 1324.
10. M. AJMAL, R. A. K. RAO and B. A. SIDDIQUI, *Wat. Res.* **30** (1996) 1478.
11. V. K. GUPTA, D. MOHAN and S. SHARMA, *Sep. Sci. Technol.* **33** (1998) 1331.
12. N. KHALID, P. O. NILORE, S. AHMAD, S. N. KIANI and J. AHMED, *ibid.* **33** (1998) 2349.
13. J. H. FORKNER, U.S. Pat. 4,042,720, 1977.

14. F. R. KUNKEL, U.S. Pat. 5,000,857, 1991.
15. M. M. DÁVILA-JIMÉNEZ, M. P. ELIZALDE-GONZÁLEZ, A. A. PELÁEZ-CID and A. ROSAS-JUÁREZ, *J. Mater. Sci. Lett.* **16** (1997) 1145.
16. M. P. ELIZALDE-GONZÁLEZ and R. RUÍZ-PALMA, *J. Chromatogr*. **845** (1999) 373.
17. G. CARRILLO-MORALES, M. M. DÁVILA-JIMÉNEZ, M. P. ELIZALDE-GONZÁLEZ and A. A. PELÁEZ-CID, *J. Chromatogr*. **938** (2001) 237.
18. M. M. DÁVILA and M. P. ELIZALDE, *Pat. Appl. Mex.* No. 041412, 1997.
19. A. L. VÁZQUEZ-DÍAZ, thesis, Universidad Autónoma de Puebla, México (1999).
20. A. V. KISELEV and V. P. DREVING, in "Eksperimental'nye metody v adsorbtsii i molekulyarnoi khromatografii" (Moscow Univ. Press, Moscow, 1973) p. 382.
21. N. V. KEL'TSEV in "Teoreticheskie Osnovy Adsorbtionnoi Tekhniki" (Khimiya, Moscow, 1976) p. 511.
22. *JCPDS ICDD*, 1991.
23. G. E. DOMBURG, V. N. SERGEEVA and A. I. KALNINSH, in "Thermal analysis," edited by H. G. Wiedemann Proceedings Third ICTA, Vol. 3 (Birkhäuser Verlag, Basel, 1972) p. 327.
24. K. V. SARKANEN, C. H. LUDWIG, in "Lignins. Occurrence, Formation, Structure and Reactions" (Wiley Interscience, New York, 1971) p. 272.
25. V. YA. DAVYDOV, A. V. KISELEV and L. T. ZHURAVLEV, *Trans. Faraday Soc*. **60** (1964) 2254.
26. S. J. GREGG and K. S. W. SING, in "Adsorption, Surface Area and Porosity" (Academic Press, London, 1982) p. 310.
27. J. HAYASHI, T. SHOJI, Y. WATADA and K. MUROYAMA, *Langmuir* **13** (1997) 4185.
28. F. ROUQUEROL, J. ROUQUEROL and K. SING, in "Adsorption by Powders & Porous Solids" (AcademicPress, London, 1999) p. 467.
29. D. P. VALENZUELA and A. L. MYERS in "Adsorption Equilibrium Data Handbook" (Prentice Hall, New Jersey, 1989) p. 364.

Received 2 November 2001
and accepted 21 November 2002